



# Type II quasar candidates in the Sloan Digital Sky Survey: evidence for X-ray obscuration

C. Vignali<sup>1,2</sup>, D.M. Alexander<sup>3</sup> and A. Comastri<sup>2</sup>

<sup>1</sup> *Dipartimento di Astronomia, Università degli Studi di Bologna, Via Ranzani 1, 40127 Bologna, Italy; e-mail: cristian.vignali@bo.astro.it*

<sup>2</sup> *INAF-Osservatorio Astronomico di Bologna, Via Ranzani 1, 40127 Bologna, Italy*

<sup>3</sup> *Institute of Astronomy, Madingley Road, Cambridge, CB3 0HA, UK*

## ABSTRACT

Recent X-ray surveys with *Chandra* and *XMM-Newton* have found several genuine Type II quasars, the long sought-after population of high-luminosity (high-redshift) Seyfert 2 galaxies, and a sizable number of Type II quasar candidates. However, at present it is hard to know whether the on-going X-ray surveys are providing a reliable and nearly complete census of the Type II quasar population. In order to address this open issue and shed light on the broad-band properties of Type II quasars, we used the sample of 291 high-ionization narrow emission-line AGN at  $z=0.3-0.83$  selected from the Sloan Digital Sky Survey by Zakamska et al. (2003). Using archival X-ray information, we were able to place constraints on the X-ray emission of 17 of these objects (three X-ray detections and 14 upper limits). Using the  $[\text{O III}]\lambda 5007$  line luminosities to predict the intrinsic X-ray power of the AGN, we found that at least 47% of the objects in the observed sample provides evidence for the presence of X-ray absorption (with  $N_{\text{H}} \gtrsim 10^{22} \text{ cm}^{-2}$ ), including the four highest luminosity sources with predicted unobscured luminosities of  $\approx 10^{45} \text{ erg s}^{-1}$ . For the only source with moderate-quality *XMM-Newton* spectral data, all of the pieces of the puzzle (2–10 keV luminosity of  $\approx 4 \times 10^{44} \text{ erg s}^{-1}$ ,  $N_{\text{H}} \approx 1-3 \times 10^{22} \text{ cm}^{-2}$ , and unobscured magnitude  $M_{\text{B}} \approx -26$ ) assure that this is a genuine Type II quasar.

## 1. INTRODUCTION

Type II quasars, the long sought-after luminous analogs of Seyfert 2 galaxies (i.e., sources with high-ionization, narrow optical emission-line spectra) predicted by Unification models of Active Galactic Nuclei (AGN), represent a key ingredient of many AGN synthesis models for the X-ray background (XRB; e.g., Comastri et al. 2001; Gilli, Salvati & Hasinger 2001). In the X-ray band these objects are expected to be highly luminous ( $\gtrsim$  a few  $\times 10^{44} \text{ erg s}^{-1}$ ) and absorbed by column densities  $\gtrsim 10^{22} \text{ cm}^{-2}$ . Before the advent of *Chandra* and *XMM-Newton*, Type II quasars formed quite an elusive class of sources. It was not rare for AGN to be mis-classified as Type II quasars

due to either limited spectral coverage or low signal-to-noise ratio optical spectra (see Halpern, Turner & George 1999). X-ray surveys conducted over the last few years have proven to be effective in finding several genuine Type II quasars (i.e., matching both the optical and X-ray definitions; e.g., Norman et al. 2002; Stern et al. 2002; Fiore et al. 2003; Gandhi et al. 2004; Caccianiga et al. 2004; Szokoly et al. 2004) and many more Type II quasar candidates (e.g., Crawford et al. 2001; Mainieri et al. 2002; Barger et al. 2003). Multiwavelength observations of these objects generally support their Type II quasar status. However, some questions regarding Type II quasars still remain without an answer despite the significant progress accomplished by X-ray surveys over the last few years, mainly *what is the fraction of genuine Type II quasars among the hard X-ray selected population?* At present, less than  $\approx 20\%$  of the hard X-ray, presumably absorbed sources, have optical counterparts matching the Type II quasar definition (e.g., Barger et al. 2003). However, in many cases the faint optical counterparts of X-ray selected Type II quasar candidates hamper the spectroscopic identification, hence providing *further uncertainty on whether or not the census of these objects from X-ray surveys is complete*. Thus, the selection of an optically bright sample can complement the information provided by X-ray surveys and shed light on the properties of the Type II quasar population as a whole.

Motivated by these considerations, we have used the sample of 291 high-ionization narrow emission-line AGN at redshift 0.3–0.83 selected by Zakamska et al. (2003, hereafter Z03) from the Sloan Digital Sky Survey (SDSS) spectroscopic data. The sample includes (in almost similar fractions) both Seyfert 2 galaxies and their higher luminosity “cousins”, Type II quasars; although not complete, this catalog represents the only published optically selected sample of Type II quasar candidates in this redshift range. Here we review the main X-ray properties of the SDSS Type II quasar candidates; a detailed analysis is presented by Vignali, Alexander & Comastri (2004).

$H_0=70 \text{ km s}^{-1} \text{ Mpc}^{-1}$ ,  $\Omega_M=0.3$ , and  $\Omega_\Lambda=0.7$  are used throughout the paper.

## 2. X-RAY DATA

The Z03 catalog of Type II quasar candidates was cross correlated with archival *ROSAT* (PSPC, HRI, and *ROSAT* All Sky Survey, RASS), *Chandra*, and *XMM-Newton* observations. Most of the data presented in the following have been obtained from *ROSAT* observations, given the larger areal coverage of archival *ROSAT* fields. We found reliable X-ray information (a detection or upper limit) for 17 sources (listed in Table 1 along with the derived X-ray parameters). One of these 17 sources was found in an archival *XMM-Newton* observation, while none of the Z03 sources lies in archival *Chandra* observations.

Overall, adopting a detection threshold of  $3.2\sigma$  ( $3.7\sigma$ ) for pointed (RASS) observations and a matching radius of  $40''$ , three sources of the Z03 sample have significant ( $\gtrsim 6\sigma$ ) X-ray detections with *ROSAT* (sources #148, #204, and #239). Source #204 was detected also by *XMM-Newton* and has enough counts for moderate-quality spectral analysis (see §4). The histogram of the [O III] line luminosities ( $L_{[O\ III]}$ ) for all of the sources in the Z03 sample is shown in Fig. 1. Note that 14 of the 17 sources with available X-ray data (filled histograms) have  $L_{[O\ III]}$  in the range  $\approx 3 \times 10^8 - 10^{10} L_\odot$ , suggesting unobscured magnitudes of  $-27 < M_B < -23$  (see Z03 for details). We are also able to provide constraints on the X-ray properties of four of the eight highest luminosity Type II quasar candidates of the Z03 sample (predicted  $L_{2-10 \text{ keV}}$  luminosities of  $\approx 10^{45} \text{ erg s}^{-1}$ ; see Fig. 1 and Tab. 1). The identification of such high-luminosity rare obscured quasars allows us to explore a different region of parameter space to that typically probed by X-ray surveys.

**Table 1.** Properties of the Zakamska et al. (2003) Type II AGN with X-ray data and constraints on the column densities.

Src <sup>a</sup> ID	SDSS J	<i>z</i>	$L_{[O\ III]}^{b}$ ( $L_{\odot}$ )	$L_{\text{HX}}^{b}$ (2–10 keV)	$F_{\text{SX}}^{c}$ (0.5–2 keV)	$N_{\text{H},z}^{d}$ Range	Type II <sup>e</sup> QSO
34	021047.01–100152.9	0.540	9.79	45.1	< 2.00	$>6.0 \times 10^{22}$ – $2.0 \times 10^{23}$	*
55	023359.93+004012.7	0.388	8.17	43.5	< 0.43	$>1.1 \times 10^{22}$ – $9.6 \times 10^{22}$	
59	024309.79+000640.3	0.414	7.95	43.3	< 0.92	$>7.0 \times 10^{21}$ – $4.9 \times 10^{22}$	
68	025558.00–005954.0	0.700	8.51	43.9	< 3.54	$>0$ – $2.0 \times 10^{22}$	
70	025951.28+002301.0	0.505	8.53	43.9	< 2.87	$>0$ – $4.7 \times 10^{22}$	
130	084234.94+362503.1	0.561	10.10	45.5	< 2.53	$>8.0 \times 10^{22}$ – $2.3 \times 10^{23}$	*
<b>148</b>	090933.51+425346.5	0.670	8.92	44.3	39.5	0	
152	092014.11+453157.3	0.402	9.04	44.4	< 2.75	$>1.3 \times 10^{22}$ – $1.0 \times 10^{23}$	*
174	100854.43+461300.7	0.544	8.32	43.7	< 3.42	$>0$ – $2.3 \times 10^{22}$	
188	104505.39+561118.4	0.428	9.08	44.4	< 3.51	$>8.5 \times 10^{21}$ – $9.5 \times 10^{22}$	*
<b>204</b>	122656.48+013124.3	0.732	9.66	45.0	2.63	$2.3 \times 10^{22}$ – $1.8 \times 10^{23}$	*
<i>f</i>				44.6	3.90	$7.5 \times 10^{21}$ – $2.0 \times 10^{22}$	*
208	123453.10+640510.2	0.594	8.77	44.1	< 4.74	$>0$ – $4.1 \times 10^{22}$	
209	124736.07+023110.7	0.487	8.59	43.9	< 3.61	$>0$ – $4.6 \times 10^{22}$	
212	130740.56–021455.3	0.425	8.92	44.3	< 8.37	$>0$ – $4.9 \times 10^{22}$	
<b>239<sup>g</sup></b>	150117.96+545518.3	0.338	9.06	44.4	30.3	$0$ – $3.0 \times 10^{23}$	
256	164131.73+385840.9	0.596	9.92	45.3	< 2.44	$>6.0 \times 10^{22}$ – $2.1 \times 10^{23}$	*
258	165627.28+351401.7	0.679	8.57	43.9	< 1.53	$>0$ – $6.2 \times 10^{22}$	

NOTE — The X-ray detected objects are shown in boldface.

<sup>a</sup> From Table 1 of Z03. <sup>b</sup> Logarithm of the predicted 2–10 keV luminosity in units of  $\text{erg s}^{-1}$ ; the relative uncertainty is  $\pm 0.6$  (i.e., the  $1\sigma$  scatter in the Mulchaey et al. 1994 correlation between the [O III] line flux and the 2–10 keV flux found for Seyfert 2 galaxies). This correlation has been applied to our data and used to predict the expected 0.5–2 keV flux for each object; see §3 for details. <sup>c</sup> Galactic absorption-corrected flux (or  $3\sigma$  upper limit) in the observed 0.5–2 keV band, in units of  $10^{-14}$   $\text{erg cm}^{-2} \text{s}^{-1}$ . <sup>d</sup> The range of column densities reported here (in  $\text{cm}^{-2}$ ) has been derived on a source-by-source basis by comparing the predicted 0.5–2 keV fluxes (using the Mulchaey et al. 1994 correlation) with the observed 0.5–2 keV fluxes (or  $3\sigma$  upper limits). For the sources that have not been detected by *ROSAT*, the column densities should be considered as lower limits (hence the use of “ $>$ ”). For the three X-ray detected sources, the column density range is broadly consistent with the absorption derived from the hardness-ratio analysis using *ROSAT* data. <sup>e</sup> \* indicates the likely absorbed sources with predicted 2–10 keV luminosities  $\gtrsim 3 \times 10^{44}$   $\text{erg s}^{-1}$ , i.e., within the Type II quasar locus. <sup>f</sup> XMM-*Newton* observation of source #204. The observed 0.5–2 keV flux and de-absorbed 2–10 keV luminosity shown here have been derived directly from X-ray spectral fitting of XMM-*Newton* data. <sup>g</sup> Detected in the RASS.

### 3. THE X-RAY PROPERTIES OF TYPE II QUASAR CANDIDATES

To derive basic constraints on the X-ray emission of the 17 Type II quasar candidates in our sample, we have used the correlation between the [O III] flux and the 2–10 keV flux found for Seyfert 2 galaxies by Mulchaey et al. (1994, hereafter M94) adopting the parameterization reported in §3.2 of Collinge & Brandt (2000). Using this approach, for each source we have predicted the expected 2–10 keV flux and errors (on the basis of the  $1\sigma$  scatter in the M94 correlation). The [OIII] line luminosities used in this work are not corrected for the absorption toward the narrow-line region (see Maiolino et al. 1998 for details). This correction would require the measurement of the Balmer decrement, but the redshift range of the Z03 sources and the bandpass of the SDSS spectra (3800–9200 Å)

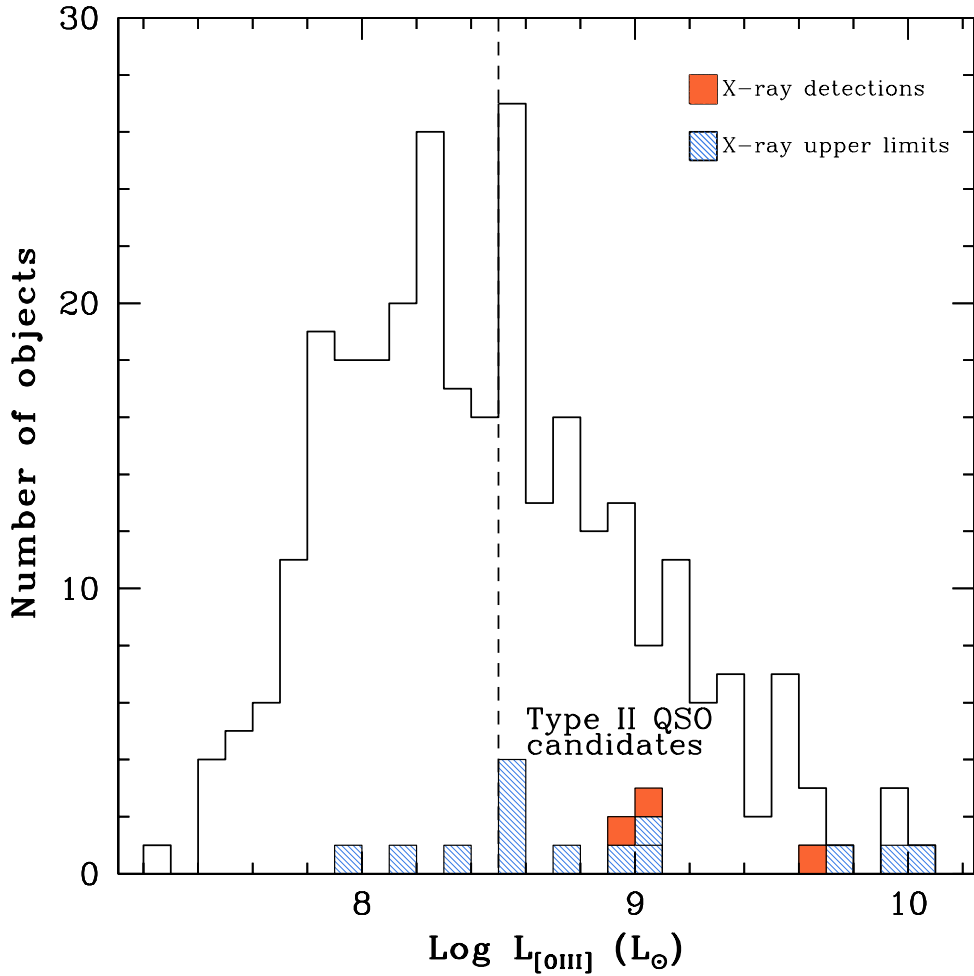


**Fig. 1.** Histogram of the [O III] line luminosities (uncorrected for absorption toward the narrow-line region) for all of the sources in the Z03 sample (thick solid line). The  $L_{[O\ III]}$  distributions for the sources with either X-ray upper limits or detections are shown as filled histograms. The locus to the right of the vertical dashed line is populated by objects having [O III] line luminosities in the range  $\approx 3 \times 10^8$  to  $10^{10} L_{\odot}$ , suggesting unobscured magnitudes of  $-27 < M_B < -23$  (see Z03 for details).

do not provide spectral coverage of the H $\alpha$  line for all of the objects. We note that using the uncorrected [OIII] line flux leads to a conservative determination in whether or not a source is absorbed in the X-ray band.

The predicted 2–10 keV fluxes (with their  $1\sigma$  uncertainties) have been converted into soft (0.5–2 keV) X-ray fluxes assuming a power law with photon index  $\Gamma=2$ , which is a relatively good parameterization of the intrinsic X-ray continua of both Type I and Type II AGN (e.g., Nandra & Pounds 1994; Risaliti 2002). These predicted soft X-ray

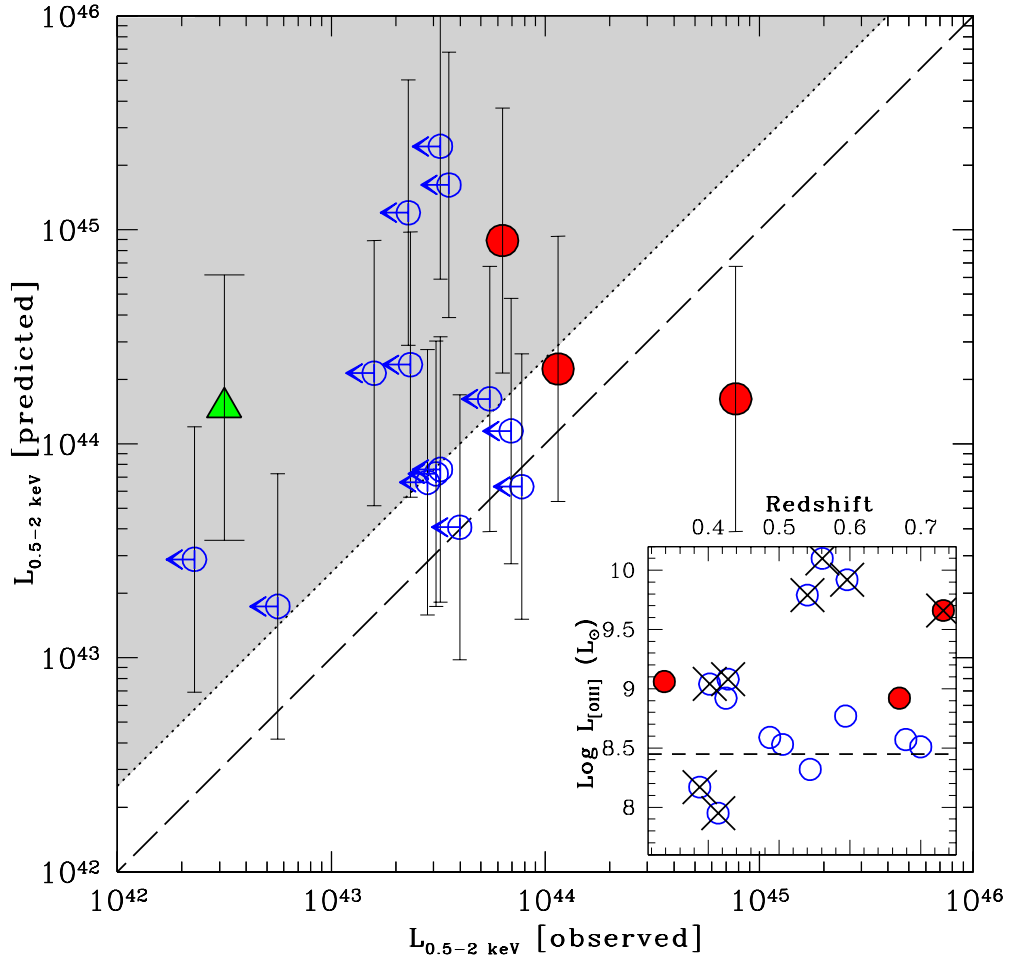


**Fig. 2.** Predicted vs. observed soft X-ray luminosity for the Z03 objects with archival X-ray observations. The filled circles indicate the three X-ray detections (two from pointed observations and one from the RASS); the filled triangle shows the result from X-ray stacking analysis of all X-ray undetected objects (individually shown as open circles). Note the large X-ray luminosity for the rightmost object (source #148) of the plot; this is also the most radio-loud source of the entire Z03 catalog. The dashed diagonal line shows the 1:1 correlation, while the dotted line indicates the correlation expected for a source at  $z=0.5$  if the column density is  $10^{22} \text{ cm}^{-2}$ . The grey region shows the locus of likely absorbed ( $N_{\text{H}} > 10^{22} \text{ cm}^{-2}$ ) sources. The column densities associated with our objects, given the method used for their derivation, should be considered conservative (see §3 for details). In the inset, the  $L_{[\text{O III}]}$  vs. redshift is plotted for the objects with X-ray observations. The crosses indicate the likely absorbed objects (see Table 1). As in Fig. 1, objects above the dashed line have  $[\text{O III}]$  line luminosities typical of unobscured quasars ( $-27 < M_{\text{B}} < -23$ ).

fluxes have then been compared to the observed soft X-ray fluxes (or the  $3\sigma$  upper limits for the X-ray non-detections; see Table 1). This allows us to estimate on a source-by-source basis the amount of X-ray absorption (listed as a range in Table 1 due to the scatter in the M94 correlation) required to produce the predicted soft X-ray flux. The principal, basic assumption used to derive the X-ray column densities is that these Type II quasar candidates have the same underlying average X-ray continua of local AGN. Clearly, the uncertainties associated with the predicted soft X-ray fluxes (and thus with the derived column densities) are large, mostly due to the scatter in the M94 correlation and partly due to the assumed underlying X-ray spectral slope. Intrinsically flatter X-ray spectral slopes would produce lower column densities (by  $\approx 20\%$ , if  $\Gamma=1.6$  instead of 2.0 is adopted), while the presence of an additional soft X-ray component (e.g., thermal emission from the host galaxy, scattering, etc.), often observed in hard X-ray selected sources (e.g., Vignali et al. 2001) would produce the opposite effect. However, within the assumptions adopted in this study, these column densities should be treated as lower limits, since all but three of our sources are not detected in the soft X-ray band.

Using the approach described above, we have found that at least 47% (8/17) of the sources with X-ray information indicate the presence of X-ray absorption (see Fig. 2 and Table 1), with column densities typically  $\gtrsim 10^{22} \text{ cm}^{-2}$  (dotted line in Fig. 2 for a source at  $z=0.5$ ). The predicted 2–10 keV luminosities of six of the eight likely absorbed sources place them in the quasar regime ( $L \gtrsim 10^{44.4} \text{ erg s}^{-1}$ ; see Table 1). Furthermore, the four most luminous sources ( $L \approx 10^{45} \text{ erg s}^{-1}$ ; see Table 1) in the sample show evidence for obscuration at X-ray energies. A column density of  $\approx 1-3 \times 10^{22} \text{ cm}^{-2}$  was obtained for source #204 through direct X-ray spectral analysis of *XMM-Newton* data (see §4).

For the 14 X-ray undetected sources we performed a stacking analysis, obtaining an  $\approx 4\sigma$  detection (triangle in Fig. 2). Although the statistical relevance of this detection is poor, the comparison of the average flux derived from the stacking analysis (weighted by the exposure time of each observation with respect to the total) with that expected on the basis of the M94 correlation provides an average column density of  $1.4-2.7 \times 10^{23} \text{ cm}^2$ . Hopefully, tighter constraints will be obtained soon with the scheduled observations of some of the most luminous Type II quasar candidates with *Chandra*.

#### 4. THE X-RAY SPECTRUM OF A GENUINE TYPE II QUASAR

Source #204 ( $z=0.732$ ) has been serendipitously observed and detected by *XMM-Newton* (see Fig. 3 for the combined pn+MOS1+MOS2 image), with a total number of  $\approx 510$  counts in the 0.5–10 keV band. A simple power-law model provides a poor fit to the *XMM-Newton* data ( $\chi^2/\text{d.o.f.}=61.2/32$ ); the derived flat photon index ( $\Gamma=0.74^{+0.12}_{-0.13}$ ) suggests the presence of absorption. If absorption at the source redshift is added to the power-law model, the fit improves significantly ( $\Delta\chi^2=16$ ); the best-fitting spectrum (shown in Fig. 4, left panel) is parameterized by a photon index  $\Gamma=1.30^{+0.16}_{-0.24}$  and a column density  $N_{\text{H}}=1.20^{+0.75}_{-0.51} \times 10^{22} \text{ cm}^{-2}$ . The 68, 90, and 99% confidence contours for the photon index vs. column density are shown in Fig. 4 (right panel). If the photon index is forced to be  $\Gamma=1.8-2.0$ , more representative of the typical AGN intrinsic X-ray emission,  $N_{\text{H}}$  becomes  $2.2-3.2 \times 10^{22} \text{ cm}^{-2}$ , more consistent with the lower column density boundary derived from *ROSAT* data (see Table 1). We note, however, that variability in the column density might have occurred between the *ROSAT* and *XMM-Newton* observations (over a time-scale of  $\approx 10$  yr). The intrinsic 2–10 keV luminosity ( $10^{44.6} \text{ erg s}^{-1}$ ), the column density ( $\approx 1-3 \times 10^{22} \text{ cm}^{-2}$ ), the narrow-line optical spectrum (Z03), and the predicted unobscured absolute *B*-band magnitude ( $\approx -26$ ) are fully consistent with source #204 being a genuine Type II quasar.

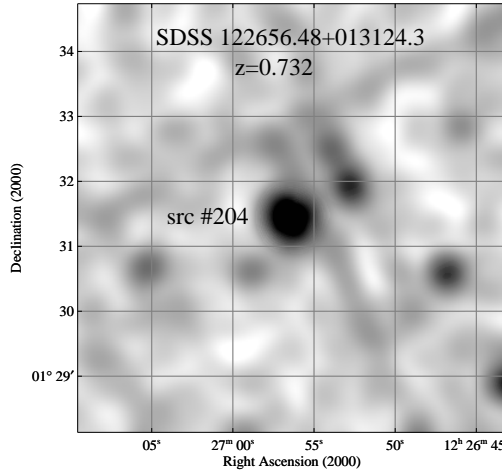


**Fig. 3.** Adaptively smoothed XMM-Newton EPIC (pn+MOS1+MOS2) image centered on source #204. The box size is  $\approx 400'' \times 400''$ . North is up, and East is to the left.

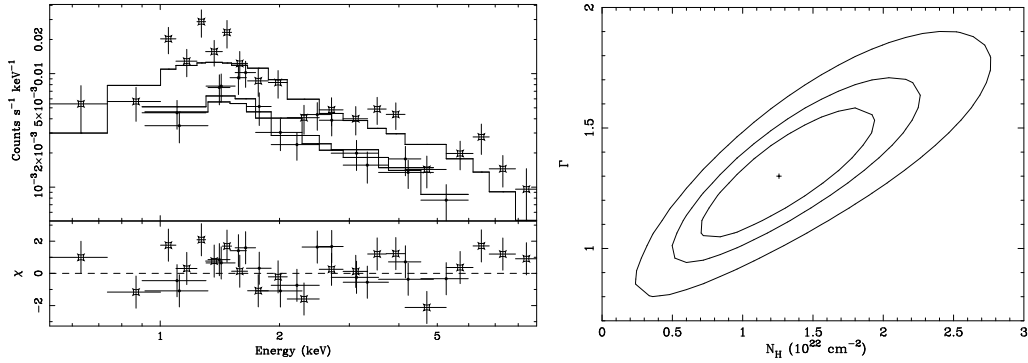


**Fig. 4.** XMM-Newton data of source #204. Left panel: pn (larger open symbols) and MOS1+MOS2 (small filled circles) spectral data (top panel) and data/model residuals (bottom panel, in units of  $\sigma$ ). Right panel: 68, 90, and 99% confidence contours for the photon index vs. intrinsic column density.

## 5. SUMMARY

We have derived basic X-ray constraints for 17 Type II (high-ionization, narrow emission-line) quasar candidates at  $z=0.3-0.83$  selected from the SDSS.

- (a) At least 47% (8/17) of the sources in the present sample indicate the presence of absorption, with column densities  $\gtrsim 10^{22} \text{ cm}^{-2}$ . In particular, there are indications that the four highest luminosity objects ( $L_{2-10 \text{ keV}} \approx 10^{45} \text{ erg s}^{-1}$ ) are absorbed. The study of such objects is important since it allows the exploration of a different part of parameter space to that typically probed by X-ray surveys.
- (b) X-ray spectral fitting of moderate-quality XMM-Newton data for source #204 provides direct evidence of intrinsic absorption, with a column density of

$\approx 1-3 \times 10^{22} \text{ cm}^{-2}$ . This result, coupled with the intrinsic 2–10 keV luminosity of  $\approx 10^{44.6} \text{ erg s}^{-1}$ , the presence of luminous high-ionization and narrow optical lines, and the unobscured magnitude  $M_B \approx -26$  makes this source a genuine Type II quasar at optical and X-ray wavelengths.

Our results complement those obtained recently by Zakamska et al. (2004) on the basis of lower significance RASS data. In particular, Zakamska et al. (2004) noticed that the fraction of SDSS Type I AGN at  $z=0.3-0.8$  with a RASS counterpart is much higher than that of SDSS Type II AGN. This result is suggestive of suppression of soft X-rays by  $N_H \gtrsim 10^{22} \text{ cm}^{-2}$  in the Type II sources.

Investigations of larger samples of SDSS Type II quasars with *Chandra* and XMM-*Newton* are clearly required to draw a more accurate and comprehensive picture of the physical properties of this enigmatic class of AGN.

**Acknowledgements.** CV and AC acknowledge partial support by the Italian Space agency (contract ASI I/R/057/02) and MIUR (COFIN grant 03-02-23). DMA is supported by the Royal Society. The authors would like to thank L. Angeretti for help in producing the plots.

## REFERENCES

Barger, A.J., et al. 2003, AJ, 126, 632  
 Caccianiga, A., et al. 2004, A&A, 416, 901  
 Collinge, M.J., & Brandt, W.N. 2000, MNRAS, 317, L35  
 Comastri, A., Fiore, F., Vignali, C., Matt, G., Perola, G.C., & La Franca, F. 2001, MNRAS, 327, 781  
 Crawford, C.S., Fabian, A.C., Gandhi, P., Wilman, R.J., & Johnstone R.M. 2001, MNRAS, 324, 427  
 Fiore, F., et al. 2003, A&A, 409, 79  
 Gandhi, P., Crawford, C.S., Fabian, A.C., & Johnstone, R.M. 2004, MNRAS, 348, 529  
 Gilli, R., Salvati, M., & Hasinger, G. 2001, A&A, 366, 407  
 Halpern, J., Turner, T.J., & George, I.M. 1999, MNRAS, 307, L47  
 Mainieri, V., Bergeron, J., Hasinger, G., Lehmann, I., Rosati, P., Schmidt, M., Szokoly, G., & Della Ceca, R. 2002, A&A, 393, 425  
 Maiolino, R., Salvati, M., Bassani, L., Dadina, M., Della Ceca, R., Matt, G., Risaliti, G., & Zamorani, G. 1998, A&A, 338, 781  
 Mulchaey, J.S., Koratkar, A., Ward, M.J., Wilson, A.S., Whittle, M., Antonucci, R.R.J., Kinney, A.L., & Hurt, T. 1994, ApJ, 436, 586 (M94)  
 Nandra, K., & Pounds, K.A. 1994, MNRAS, 268, 405  
 Norman, C., et al. 2002, ApJ, 571, 218  
 Risaliti, G. 2002, A&A, 386, 379  
 Stern, D., et al. 2002, ApJ, 568, 71  
 Szokoly, G.P., et al. 2004, ApJS, in press (astro-ph/0312324)  
 Vignali, C., Comastri, A., Fiore, F., & La Franca, F. 2001, A&A, 370, 900  
 Vignali, C., Alexander, D.M., & Comastri, A. 2004, MNRAS, in press (astro-ph/0407293)  
 Zakamska, N.L., et al. 2003, ApJ, 126, 2125 (Z03)  
 Zakamska, N.L., Strauss, M.A., Heckman, T.M., Ivezic, Z., & Krolik, J.H. 2004, AJ, 128, 1002